



In vivo release from a drug delivery MEMS device

Yawen Li^a, Rebecca S. Shawgo^a, Betty Tyler^b, Paul T. Henderson^c, John S. Vogel^c,
Aron Rosenberg^a, Phillip B. Storm^b, Robert Langer^d, Henry Brem^b, Michael J. Cima^{a,*}

^aDepartment of Materials Science and Engineering, Massachusetts Institute of Technology, Cambridge, MA 02139, United States

^bDepartment of Neurological Surgery, Johns Hopkins University School of Medicine, Baltimore, MD 21205, United States

^cBiology and Biotechnology Research Program and Center for Accelerator Mass Spectrometry, Lawrence Livermore National Laboratory, Livermore, CA 94551, United States

^dDepartment of Chemical Engineering, Massachusetts Institute of Technology, Cambridge, MA 02139, United States

Received 22 June 2004; accepted 25 August 2004

Available online 28 September 2004

Abstract

A drug delivery microelectromechanical systems (MEMS) device was designed to release complex profiles of multiple substances in order to maximize the effectiveness of drug therapies. The device is based on micro-reservoirs etched into a silicon substrate that contain individual doses of drug. Each dose is released by the electrochemical dissolution of the gold membrane that covers the reservoir. The first in vivo operation of this device was reported in this study. Subcutaneous release was demonstrated in rats using two tracer molecules, fluorescein dye and radiolabeled mannitol, and one radiolabeled chemotherapeutic agent, carmustine (BCNU). BCNU was chosen because of the need to improve the direct delivery of chemotherapy to malignant tumors. The spatial profile of fluorescein dye release from the drug delivery device was evaluated by fluorimetry, the temporal profile of ¹⁴C labeled mannitol release was evaluated by liquid scintillation counting, and the temporal profile of ¹⁴C labeled BCNU release was evaluated by accelerator mass spectrometry (AMS). Release profiles obtained from injected controls were compared with those from activated devices. The in vivo dye release results showed high concentration of fluorescein in the flank tissue surrounding the devices 1 h after activation. The ¹⁴C labeled mannitol released from the drug delivery devices was rapidly cleared (1 day) from the rat urine. In vivo release of ¹⁴C labeled BCNU from activated devices showed slightly slower kinetics than the injected and in vitro controls, and the time to reach the steady-state plasma ¹⁴C concentration was on the order of 1 h. All these results demonstrated the capability of this drug delivery device to achieve localized delivery of various compounds with well-defined temporal profiles.

© 2004 Elsevier B.V. All rights reserved.

Keywords: Microelectromechanical systems (MEMS); Drug delivery; In vivo release kinetics; Carmustine (BCNU); Accelerator mass spectrometry (AMS)

* Corresponding author. Tel.: +1 6172536877; fax: +1 6172586936.

E-mail address: mjcima@mit.edu (M.J. Cima).

1. Introduction

Most controlled release implants are capable of delivering only a single compound at a constant rate although it is well known that the rate of a drug's delivery and its interactions with other chemicals have a significant influence on its effectiveness [1]. Recent advances in the fabrication of microelectromechanical systems (MEMS) offer unique opportunities to create novel implantable drug delivery systems to maximize the efficacy of drug therapies [2,3]. A variety of microfabricated devices and components have been designed to release drugs of different dosages and with different delivery pattern and duration to address various clinical needs. For example, microfluidic devices that incorporate micropumps, valves and flow channels have been investigated to deliver drugs, proteins and genes [4,5]. Microfabricated porous membranes have been used for drug encapsulation [6] and microparticles have been used for aerosol and gene delivery [7,8].

An implantable drug delivery MEMS device has been developed that is capable of delivering multiple substances either in series or in parallel [9]. The device is based on a silicon substrate into which micro-reservoirs are etched. Each reservoir is filled with a dose of drug and covered with a gold membrane (Fig. 1). The membrane electrochemically corrodes into soluble gold chloride when a positive potential is applied, and the drug in the reservoir is free to dissolve or diffuse into solution [10]. Potential advantages of this device include the variety of deliverable compounds, capability of complex release profiles, and precise dosing. Limitations include the small size of the micro-reservoirs and the need for surgical implantation and explantation. This kind of device may be particularly useful for the delivery of hormones, powerful painkillers, chemotherapeutic drugs, and other potent drugs.

One such compound of potential use is 1,3-bis(2-chloroethyl)-1-nitrosourea (BCNU), otherwise known as carmustine, an alkylating agent that binds DNA to form interstrand cross-links. Biodegradable polymers incorporated with BCNU (Gliadel®) have been used for the sustained release of BCNU for brain tumor therapy. Although Gliadel has prolonged survival for brain tumor patients, the tumors eventually progress causing death [11]. Local delivery of BCNU com-

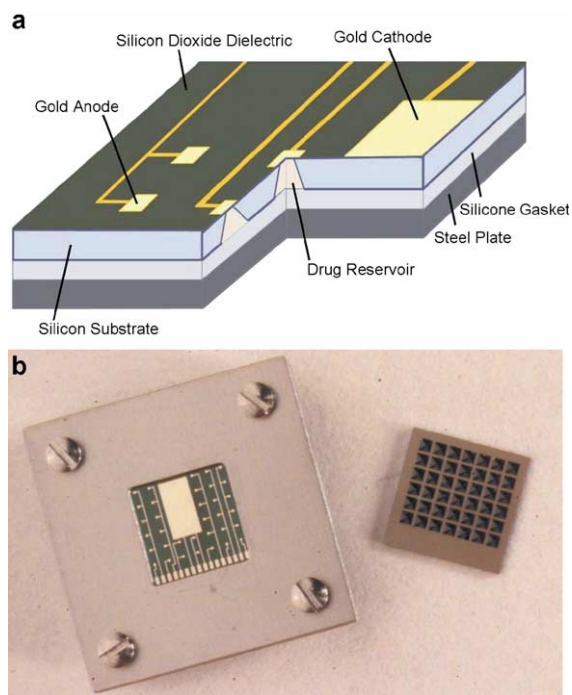


Fig. 1. (a) Schematic of drug delivery MEMS device and (b) photograph showing a packaged device and the reservoirs of a device.

bined with other chemotherapeutic agents, such as O⁶-benzylguanine, or immunotherapeutic agents, such as interleukin-2, can enhance the efficacy of BCNU therapy. Laboratory studies have indeed demonstrated improved survival on experimental tumor models [12,13]. Effective delivery of the multi-drug combination requires precise control of the temporal and spatial profiles of the agents, which is generally difficult to achieve using biodegradable polymers. A MEMS drug delivery device, on the other hand, will enable release of multiple compounds in complex release profiles to maintain drug concentrations within their therapeutic window. Moreover, the impermeable gold membranes can effectively protect the drugs contained in the microreservoirs from hydrolytic degradation before release. It is likely that the same therapeutic effect can be achieved using the MEMS device with lower drug dosage requirement compared to the drug impregnated polymer wafers so that systemic toxicities will be decreased.

Understanding the release kinetics of BCNU from this drug delivery device is important for its *in vivo* operation. Available pharmacokinetic data using ¹⁴C

labeled BCNU indicate that the compound and its metabolites are accumulated in the liver, kidney and lungs, and that approximately 78% of a radioactive dose injected intraperitoneally, subcutaneously, or taken orally, is excreted from mice within 24 h. The plasma ^{14}C concentration, though only a small portion (1–5%) of the dose, remains constant in the plasma for relatively long duration with a 67-h half life [14]. It is therefore appropriate to measure pulses of BCNU release from the drug delivery device using plasma samples to obtain the temporal release kinetics. This approach however is limited by the relatively low sensitivity of the conventional liquid scintillation counting (LSC) with respect to the low plasma ^{14}C level. An alternative tool of isotope detection is the accelerator mass spectrometry (AMS), a highly sensitive method for quantifying extremely low concentrations of radioisotopes with ultrahigh precision [15,16]. Additional advantages of AMS include low radioactivity and small sample size requirements.

2. Materials and methods

2.1. General procedure

A two-part study examined the release of chemical substances from a drug delivery MEMS device. First, the release of two tracer molecules was studied on devices implanted subcutaneously in rats. A voltammetric profile sufficient to activate the device *in vivo* was established; the spatial profile of fluorescein release and temporal profile of mannitol release were examined. The second part of the study examined the temporal release kinetics of ^{14}C labeled BCNU from devices.

2.2. Device fabrication and packaging

The device fabrication followed the same process as described elsewhere [9]. Devices were filled with solutions of PEG 200, sodium fluorescein, or ^{14}C labeled BCNU (Moravek Biochemicals, Brea, CA) using a microinjector (UltraMicroPump II, World Precision Instruments, Sarasota, FL). PEG (MW: 200) gel was used to reduce the drying stress on the membranes. ^{14}C labeled mannitol was loaded into devices as solid pieces. Devices were packaged into

stainless steel frames with either silicone gaskets (Advanced Bio-Technologies, Silverdale, WA) or neoprene gaskets (McMaster-Carr Supply, Los Angeles, CA) to seal the micro-reservoirs. Wirebonds connected the bondpads on the device to connector boards and Teflon coated cables. Wirebonds were mechanically protected and electrically isolated with epoxy (Masterbond EP42HT, Hackensack, NJ). Silver or platinum wire was used as an *in vivo* reference electrode [17,18].

2.3. *In vivo* release study

Animals were housed and treated in accordance with the policies and principles of laboratory care of the Johns Hopkins University School of Medicine Animal Care and Use Committee. Rats (Fisher 344) were purchased from Charles River. Before all surgical procedures, the animals were anesthetized with an intraperitoneal injection of a stock solution containing ketamine hydrochloride (25 mg/ml), xylazine (2.5 mg/ml), and 14.25% ethyl alcohol in normal saline.

2.3.1. Fluorescein release

Devices for the release of sodium fluorescein were implanted subcutaneously with the electrodes facing the left anterior flank in 175 g female rats. An incision was made to expose the ends of the cables so that connection could be made via alligator clips to a potentiostat (Gamry PC4-300, Warminster, PA). A silver wire was used as the voltage reference. Sets of reservoir membranes were activated with various voltammetric profiles. These included cathodic cleaning cycles between -1.0 and -2.0 V, Evans scans from 0 to 1.5 V, and square wave voltammetry with a frequency of 1 Hz between 0 and 1.1 V. Devices remained in position for 1 h after activation to allow the reservoir contents to diffuse into the tissue. The animals were then sacrificed and their flanks were sectioned. Some sections were placed in tissue solvent (Solvable, Packard Bioscience, Meriden, CT) and the fluorescein content in the section determined by fluorimetry of the solution; other sections were examined with fluorescent microscopy. Controls included animals with no device, with an unactivated device, with subcutaneously injected fluorescein and also the contralateral flank of each animal.

2.3.2. Mannitol release

Devices for the mannitol release study were implanted subcutaneously in the flank of female rats (150–175 g). Rats were individually housed in metabolic cages (Nalgene model number 650-0100, Braintree Scientific, Braintree, MA) to allow for the collection of urine and feces. Device activation was modified based on the results from the fluorescein release. Cathodic cleaning from -1.0 to -1.5 V, Evans cyclic voltammetry from 0 to 1.8 V, and square wave voltammetry between 0.1 and 1.4 V, all using the Ag wire reference electrode, were performed for membrane opening. Activations were performed at 50 and 100 h after implantation. Urine samples were collected for each rat housed individually in metabolic cages. The ^{14}C level for each urine sample was measured on a liquid scintillation counter (Beckman Coulter, Fullerton, CA). Feces were not analyzed after an initial trial showed no radioactivity recovered. Controls included animals with an unactivated device and two devices that were filled but not packaged or sealed. These two unpackaged devices were implanted with the mannitol release direction facing the muscle, which is the same as for the activated device.

2.3.3. BCNU release

Female rats (150–200 g) in the BCNU release study had catheters inserted into the femoral artery that were used to remove blood samples and inject sterile saline. The devices were implanted subcutaneously with the electrodes facing the anterior flank and the cable exiting through the incision 24 h before activation. Activations were performed on three devices at 3 -h intervals. Controls included animals with an unactivated device, with subcutaneously injected ^{14}C labeled BCNU, and two devices activated *in vitro* in saline. Blood samples of $100\ \mu\text{l}$ were taken every 20 to 30 min thereafter. Sterile saline with 10% heparin was injected through the catheters after taking each blood sample to replace the blood volume lost as well as to keep the catheters from clogging. The catheterization procedure was problematic until the technique could be perfected as two rats expired before completing all the scheduled activations. Blood samples were centrifuged at 6000 rpm for 5 min to yield approximately $75\ \mu\text{l}$ plasma for each sample. The plasma ^{14}C concentration was measured by AMS,

as described below. Device activation was the same as in the mannitol release except that a platinum wire was used as the reference electrode and the square wave voltammetry was performed between 0.2 and 1.4 V.

2.3.4. AMS analysis of plasma ^{14}C concentration

The ^{14}C determinations were made at the Center for Accelerator Mass Spectrometry at Lawrence Livermore National Laboratories (Livermore, CA) as described previously [19]. Briefly, plasma samples were thawed at room temperature, vortexed and centrifuged in order to obtain a homogeneous liquid sample. A $25\ \mu\text{l}$ aliquot of each sample was placed in a quartz tube and dried by vacuum centrifuge. The sample was converted to CO_2 by combustion, and was quantitatively reduced to graphite in the presence of zinc and titanium hydride condensing onto catalytic iron at $\sim 500\ ^\circ\text{C}$ for 4 h [20]. The graphite samples were introduced into the spectrometer for three to seven replicate measurements to a precision of 3% or better. All measurements were normalized to similarly prepared standards of known carbon isotope ratios, as described elsewhere [21]. Excess ^{14}C concentrations over natural abundance were converted to plasma concentration of ^{14}C (fCi/ μl) by multiplying the measured ratio of ^{14}C to total carbon times the percent plasma carbon content. Total percent carbon in the blood plasma was measured with an Exeter CE-440 elemental analyzer (Exeter Analytical, Chelmsford, MA) to 3.28% (± 0.63), as determined in selected samples taken throughout each experiment.

3. Results

3.1. Fluorescein and mannitol release

The voltammetric profile necessary to activate the devices *in vivo* differs from that in saline because proteins adsorb onto the gold surface *in vivo* and therefore slow corrosion kinetics. Different voltammetric profiles were applied in the fluorescein release study to test their efficiency of opening anode gold membranes *in vivo*. Optical microscopy examination of the explanted devices showed that the most reliable membrane opening occurred with both a cathodic cleaning cycle and a 20 -min square wave cycle (twice

that used for the *in vitro* release), with 75% of the activated membranes fully opened and the remaining membranes partially opened. This is in contrast to the 0% of the membranes that were not cathodically cleaned and 25% of the membranes that were corroded for only 10 min.

Fig. 2 shows the tissue section fluorimetry profiles from two devices activated using the correct protocol. The profiles from an injected control and an unactivated device were also shown for comparison. The device which had purposefully more opened membranes had a greater area under the curve per membrane opened and a release profile not centered on the device position. More fluorescein was found in the posterior than in the anterior. The electrical leads ran from the device through the incision to the potentiostat in the posterior direction so diffusion may have been greater in that direction due to the surgical trauma. The other device, however, showed a nearly symmetrical distribution of fluorescein. Concentrations observed for the control with injected fluorescein were found to be lower than for the animals with activated devices.

Subcutaneous delivery by injection allows the dye to diffuse out of the tissue more rapidly and enter the systemic circulation. The animal had grossly detectable amounts of fluorescein in its urine within 5 min of injecting the fluorescein subcutaneously. In contrast, visibly detectable fluorescein was observed approximately 1 h after activation of the device. The contralateral flank of each animal was used as a negative control and exhibited only background fluorescence.

Fig. 3 shows the temporal profile of *in vivo* mannitol release evaluated by LSC analysis of the urine ^{14}C levels. Excretion of ^{14}C labeled mannitol from both the activated device and unpackaged devices was completed within 24 h. The micro-reservoirs on the drug delivery device are of square pyramidal shape. The opening for mannitol release on the unpackaged devices is about 100 times that on the activated device. Nevertheless, no difference in the mannitol release rate was detected, implying rapid release of highly soluble agents such as mannitol from the drug delivery device. About 40% of the initial ^{14}C loading was recovered in urine.

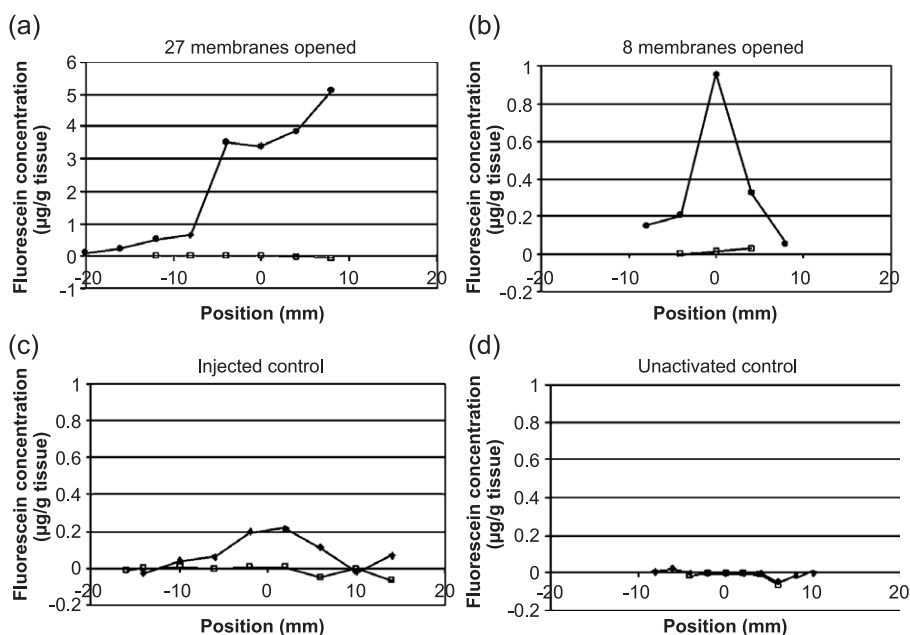


Fig. 2. The spatial release profiles of fluorescent dye measured using spectrophotometry in tissue sections from the ipsilateral (solid circle labeled) and contralateral flanks (empty square labeled) of rats. Animals had activated devices with (a) 27 and (b) 8 opened membranes, or (c) injected dye, and (d) an unactivated device. The area under the curve per reservoir emptied was (a) 2.20 and (b) 1.27 $\mu\text{g/g}$ tissue.

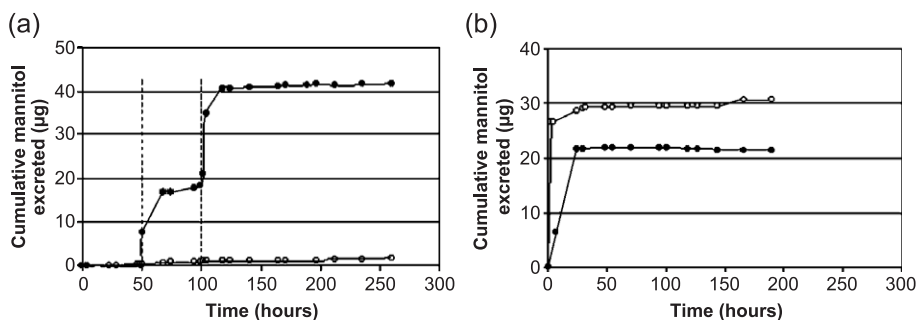


Fig. 3. Cumulative ^{14}C -mannitol excreted from (a) packaged and (b) unpackaged devices measured by LSC of the urine samples. Packaged devices contained 100 μg mannitol; unpackaged devices contained 67 μg (solid circle labeled) and 74 μg (empty circle labeled), respectively. One device in (a) was activated at 50 and 100 h after implantation (denoted by hatched lines), and the other device (empty circle labeled) acted as an unactivated control.

3.2. BCNU release

Six activations, each corresponding to the opening of one row of three or four reservoirs with a total loading of 0.01 μCi ^{14}C per row, were performed on three rats. Five out of these six activations were successful with all of the membranes opened, as

confirmed by the optical microscopy observation of the explanted devices. The unsuccessful activation was due to faulty wiring on a single row of one device. Fig. 4 shows the temporal profile of in vivo BCNU release evaluated by AMS analysis of the plasma ^{14}C concentration of the blood samples from all successful activations. The plasma ^{14}C concentration remained at

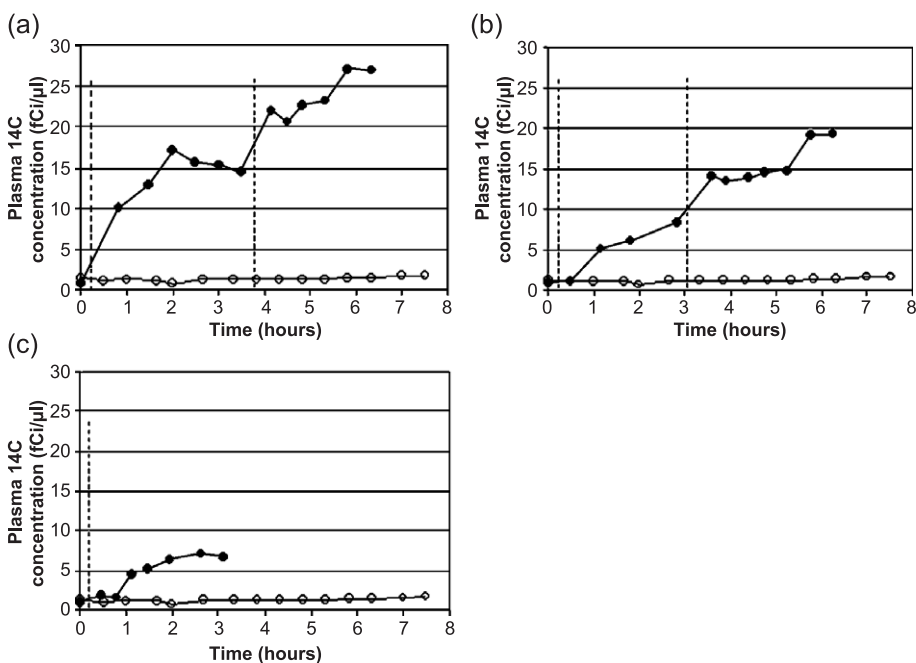


Fig. 4. Plasma ^{14}C concentration measured by AMS from devices activated in vivo, with two sequential activations in (a) and (b), and one activation in (c). Plasma ^{14}C concentration from an unactivated device is plotted in each graph (empty circle labeled) as controls. Each activation (denoted by the hatched line) corresponds to opening of one row of reservoirs with 0.01 μCi loading. Each data point represents means of 3–7 replicate measurements with 25 μl plasma sample.

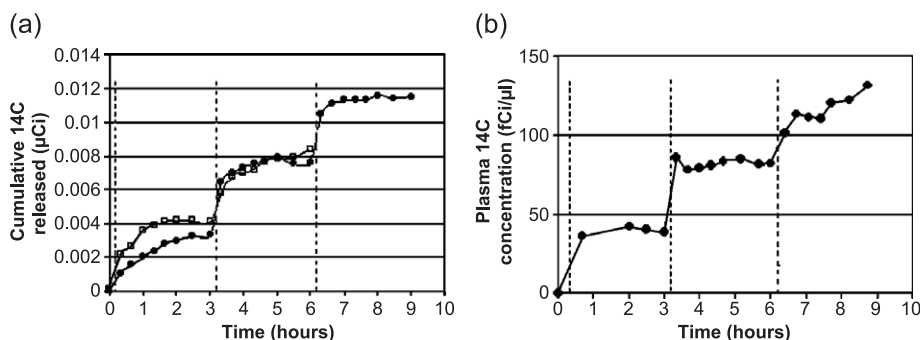


Fig. 5. (a) Cumulative ^{14}C released from devices activated in vitro in saline. Each activation (denoted by the hatched line) corresponds to opening of one row of reservoirs with $0.01\ \mu\text{Ci}$ loading. (b) Plasma ^{14}C concentration measured by AMS from a subcutaneous injected control. Each injection (denoted by the hatched line) corresponds to $0.014\ \mu\text{Ci}$ loading. Each data point represents means of 3–7 replicate measurements with $25\ \mu\text{l}$ plasma sample.

the background level following the unsuccessful activation on one rat and was not shown in Fig. 4.

All successful activations led to a sharp increase in the plasma ^{14}C concentration followed by a plateau, which is similar to both the in vitro and injected controls (Fig. 5). The ^{14}C level reached equilibrium almost instantaneously after each activation for the in vitro controls. It took about half an hour to reach the plateau plasma ^{14}C concentration for the injected control, and slightly longer for the rats with activated devices.

4. Discussion

The results of this study indicate that the subcutaneous use of this drug delivery MEMS device for delivery of drug is feasible and that the in vivo chemical release was successful. The capability of this device to achieve localized delivery of various compounds with well-defined temporal profiles was demonstrated.

A sufficient voltammetric profile for in vivo activation and complete opening of the device anode membranes was determined. This profile included a cathodic cleaning cycle to remove the surface oxide and adsorbed organics, a diagnostic cyclic (Evans) scan to characterize the corrosion and depassivation potential regions, and a square wave cycle to efficiently corrode the gold membrane. Both cathodic cleaning and longer voltammetry times were necessary in vivo to insure reproducible membrane opening. On the other hand, later in vitro results using this

device have shown that when the upper potential of the square wave cycle was increased, the length of time necessary for complete membrane opening was decreased. This is believed to be correlated with the transient formation and breakdown of a passive film, which exerts high compressive stress to the gold membrane and accelerates its disintegration. A 20-min square wave was necessary in the fluorescein release experiment for complete opening of the anode gold membranes. The activation voltage was increased for the mannitol and BNCU release so only a 10-min square wave cycle was used.

The similarity in the shape of the ^{14}C labeled BCNU release profiles between the activated devices in vivo and both the in vitro and injected controls implies that the pharmacokinetics dominated the release kinetics in all cases. The time to reach the steady-state plasma ^{14}C concentration was on the order of 1 h. The diffusion of ^{14}C labeled BCNU from the activated devices in vivo also played a role by prolonging the drug clearance time in the blood. Comparison of Fig. 5a with Fig. 4 shows that the intrinsic release rate from an activated device in vitro was faster than the distribution rate from an activated device in vivo. Clearly, the limiting resistance for in vivo distribution is external to the device. Comparison of Fig. 5b with Fig. 4 shows that more rapid distribution of BCNU occurred from the injected control than from activated devices. The drug was diluted in saline solution just before injection, but was mixed with the polyethylene glycol (PEG) gel in the reservoirs before activation. The difference in the

release rate between the activated MEMS device and the injected control indicated that transport from a 50 μm opening into surrounding tissue was intrinsically slower than transport from a solution bolus delivered by injection.

It is also noted that the plasma ^{14}C concentration of the injected control was about three to five times higher than that of the rats with activated devices, even though the ^{14}C dosing of each injection was only 1.4 times the loading for each activation of the devices. An incomplete retrieval of the filled radioactivity was found from the *in vitro* controls (Fig. 5a). All the membranes filled with the ^{14}C labeled compound were opened after activation, but only 40% of the filled loading was collected from the release medium. The remaining 60% was recovered by subsequently soaking the unpackaged devices in saline. The small molecule BCNU (MW: 214) could have been trapped in the package, most likely in the neoprene gasket and/or the epoxy. There could also be small air bubbles left in the filled reservoirs. These air bubbles could prevent the drug from completely diffusing out even when the membranes were opened. The equilibrium plasma ^{14}C concentration after the first successful activations was about the same for two rats, but was nearly twice that value for the other rat with an activated device. This interindividual variability is probably due to the variability in the drug disposition between these animals, which may be correlated with the low partition and hence the low bioavailability of the drug in blood. Higher than tenfold interpatient variation in the blood level of BCNU has been reported in the clinical study of high dose alkylators for the treatment of primary breast cancer [22].

BCNU has been known to degrade in aqueous media with a half-life of 10 to 20 min [23]. There appears to be two competing degradation mechanisms [24,25]. It can be enzymatically metabolized by the liver into an inactive form, or hydrolyzed in tissue to an active alkylating agent. BCNU has a relatively longer half-life in non-aqueous media, with 74 days in 95% ethanol [26]. Both the PEG gel and ^{14}C labeled BCNU were dissolved in ethanol for injection into the devices to avoid decomposition of the drug prior to release. Most of the measured ^{14}C in plasma probably represented the radioactivity carried by the degraded BCNU fragment, as proposed by

DeVita [14]. This could explain the rapid clearance of the plasma ^{14}C level shown in Figs. 4 and 5, although BCNU is known to be a highly lipophilic compound.

5. Conclusions

A drug delivery MEMS device was used in this study to deliver tracer molecules as well as a therapeutic agent *in vivo*. Their spatial and temporal release profiles were evaluated using fluorimetry, scintillation counting and AMS. The results clearly demonstrated the capability of this drug delivery device to achieve localized delivery of various compounds with well-defined temporal profiles. Moreover, they provided useful BCNU release kinetics information for the ongoing efficacy study that uses this device to deliver BCNU against malignant tumor challenge in a rat flank model.

Acknowledgements

This work was funded by the U.S. National Institute of Health grant no. 1 R24 AI47739-01 and U19-CA52857. R.S.S. was supported by a U.S. National Science Foundation fellowship. All micro-fabrication work was carried out at the Microsystems Technology Laboratory at MIT. The AMS work was performed under the auspices of the U.S. Department of Energy by University of California Lawrence Livermore National Laboratory under Contract W-7405-Eng-48 and in collaboration with the National Center for Research Resources GrantRR13461. The authors gratefully acknowledge Karen Dingley for many useful discussions and insights. Kurt Haack and Ester Ubeck are recognized for their work in preparing the AMS samples used in this work.

Henry Brem and the John Hopkins University own Guilford Pharmaceutical stock, which is subject to certain restrictions under University policy. Henry Brem is also a paid consultant to Guilford Pharmaceuticals. The terms of this arrangement are being managed by the John Hopkins University in accordance with its conflict of interest policies. Michael Cima and Robert Langer are shareholders in Micro CHIPS, Inc., Bedford, Massachusetts.

References

- [1] E.E. Bakken, K. Heruth, Temporal control of drugs: an engineering perspective, *Ann. N.Y. Acad. Sci.* 618 (1991) 422–427.
- [2] D.A. LaVan, T. McGuire, R. Langer, Small-scale systems for in vivo drug delivery, *Nat. Biotechnol.* 21 (10) (2003) 1184–1191.
- [3] S.Z. Razzacki, P.K. Thwar, M. Yang, V.M. Ugaz, M.A. Burns, Integrated Microsystems for controlled drug delivery, *Adv. Drug Deliv. Rev.* 56 (2) (2004) 185–198.
- [4] B. Ziaie, A. Baldi, Antonio, M. Lei, Y. Gu, R.A. Siegel, Hard and soft micromachining for BioMEMS: review of techniques and examples of applications in microfluidics and drug delivery, *Adv. Drug Deliv. Rev.* 56 (2) (2004) 145–172.
- [5] W.M. Saltzman, W.L. Olbricht, Building drug delivery into tissue engineering, *Nat. Rev. Drug Discov.* 1 (3) (2002) 177–186.
- [6] T.A. Desai, Micromachined therapeutic delivery systems: from concept to clinic, *Proc. SPIE* 4265 (2001) 26–35.
- [7] N. Tsapis, D. Bennett, B. Jackson, D.A. Weitz, D.A. Edwards, Trojan particles: large porous carriers of nanoparticles for drug delivery, *Proc. Natl. Acad. Sci. U. S. A.* 99 (2002) 12001–12005.
- [8] D. Luo, W.M. Saltzman, Synthetic DNA delivery systems, *Nat. Biotechnol.* 18 (2000) 33–37.
- [9] J.T. Santini, M.J. Cima, R. Langer, A controlled-release microchip, *Nature* 397 (1999) 335–338.
- [10] J.T. Santini, A.C. Richards, R.A. Scheidt, M.J. Cima, R. Langer, Microchips as controlled release drug delivery devices, *Angew. Chem. Int. Ed.* 39 (2000) 2396–2407.
- [11] H. Brem, S. Piantadosi, P.C. Burger, M. Walker, R. Selker, N. Vick, K. Black, M. Sisti, S. Brem, G. Mohr, P. Muller, R. Morawetz, S. Schold, Placebo-controlled trial of safety and efficacy of intraoperative controlled delivery by biodegradable polymers of chemotherapy for recurrent gliomas, *Lancet* 345 (1995) 1008–1012.
- [12] L.D. Rhines, P. Sampath, M.E. Dolan, B.M. Tyler, H. Brem, J. Weingart, O⁶-Benzylguanine potentiates the antitumor effect of locally delivered carmustine against an intracranial rat glioma, *Cancer Res.* 60 (2000) 6307–6310.
- [13] L.D. Rhines, P. Sampath, F. DiMeco, H.C. Lawson, B.M. Tyler, J. Hanes, A. Olivi, H. Brem, Local immunotherapy with interleukin-2 delivered from biodegradable polymer microspheres combined with interstitial chemotherapy: a novel treatment for experimental malignant glioma, *Neurosurgery* 52 (2003) 872–880.
- [14] V.T. DeVita, C. Denham, J.D. Davidson, V.T. Oliverio, The physiological disposition of the carcinostatic 1,3-bis(2-chloroethyl)-1-nitrosourea (BCNU) in man and animals, *Clin. Pharmacol. Ther.* 8 (1967) 566–577.
- [15] K.W. Turteltaub, J.S. Vogel, Bioanalytical applications of accelerator mass spectrometry for pharmaceutical research, *Curr. Pharm. Des.* 6 (2000) 991–1007.
- [16] J.S. Vogel, K.W. Turteltaub, R. Finkel, D.E. Nelson, Accelerator mass spectrometry: isotope quantification at attomole sensitivity, *Anal. Chem.* 67 (1995) 353A–359A.
- [17] G. Voskerician, R.S. Shawgo, P.A. Hitner, J.M. Anderson, M.J. Cima, R. Langer, In vivo inflammatory and wound healing effects of gold electrode voltammetry for MEMS micro-reservoir drug delivery device, *IEEE Trans. Biomed. Eng.* 51 (2004) 627–635.
- [18] N. Holmström, P. Nilsson, J. Carlsten, S. Bowald, Long-term in vivo experience of an electrochemical sensor using the potential step technique for measurement of mixed venous oxygen pressure, *Biosens. Bioelectron.* 13 (1998) 1287–1295.
- [19] S.D. Gilman, S.J. Gee, B.D. Hammock, J.S. Vogel, K. Haack, B.A. Buchholz, S.P. Freeman, R.C. Wester, X. Hui, H.I. Maibach, Analytical performance of accelerator mass spectrometry and liquid scintillation counting for detection of ¹⁴C-labeled atrazine metabolites in human urine, *Anal. Chem.* 70 (1998) 3463–3469.
- [20] J.S. Vogel, Rapid production of graphite without contamination for biomedical AMS, *Radiocarbon* 34 (1992) 344–350.
- [21] J.S. Vogel, A. Love, in: A.L. Burlingame (Ed.), *Methods in Enzymology*, Academic Press, New York, 2004, in press.
- [22] W.P. Petros, G. Broadwater, D. Berry, R.B. Jones, J.J. Vredenburgh, C.J. Gilbert, J.P. Gibbs, O.M. Colvin, W.P. Peters, Association of high-dose cyclophosphamide, cisplatin, and carmustine pharmacokinetics with survival, toxicity, and dosing weight in patients with primary breast cancer, *Clin. Cancer Res.* 8 (2002) 698–705.
- [23] V.A. Levin, W. Hoffman, R.J. Weinkam, Pharmacokinetics of BCNU in man: a preliminary study of 20 patients, *Cancer Treat. Rep.* 62 (1978) 1305–1312.
- [24] A. Guitani, M. Corada, C. Lucas, A. Lemoine, S. Garattini, I. Bartosek, Pharmacokinetics of fotemustine and BCNU in plasma, liver, and tumor tissue of rats bearing two lines of Walker 256 carcinoma, *Cancer Chemother. Pharmacol.* 28 (1991) 293–297.
- [25] D.L. Hill, M.C. Kirk, R.F. Struck, Microsomal metabolism of nitrosoureas, *Cancer Res.* 35 (1975) 296–301.
- [26] J.A. Montgomery, R. James, G.S. McCaleb, T.P. Johnston, The modes of decomposition of 1,3-bis(2-chloroethyl)-1-nitrosourea and related compounds, *J. Med. Chem.* 10 (1967) 668–674.